

Correlating $B_q^0 \rightarrow \mu^+ \mu^-$ and $K_L \rightarrow \pi^0 \bar{\nu} \nu$ Decays with Four Generations

Fanrong Xu^{*†}

Department of Physics, Jinan University

Guangzhou 510632, China

E-mail: fanrongxu@jnu.edu.cn

The $B_s \rightarrow \mu^+ \mu^-$ mode has finally been observed, albeit at rate 1.2σ below Standard Model (SM) value, while the rarer $B_d^0 \rightarrow \mu^+ \mu^-$ decay has central value close to 4 times SM expectation but with only 2.2σ significance. The measurement of CP violating phase ϕ_s has finally reached SM sensitivity. Concurrent with improved measurements at LHC Run 2, $K_L \rightarrow \pi^0 \nu \bar{\nu}$ and $K^+ \rightarrow \pi^+ \nu \bar{\nu}$ decays are being pursued in a similar time frame. We find, whether $B_d^0 \rightarrow \mu^+ \mu^-$ is enhanced or not, $K_L \rightarrow \pi^0 \nu \bar{\nu}$ can be enhanced up to the Grossman-Nir bound in the fourth generation model, correlated with some suppression of $B_s \rightarrow \mu^+ \mu^-$, and with ϕ_s remaining small.

The European Physical Society Conference on High Energy Physics

22–29 July 2015

Vienna, Austria

^{*}Speaker.

[†]I would like to thank my collaborators Geroge Wei-Shu Hou and Masaya Kohda .

1. Introduction

The 7-and-8 TeV run (Run 1) of the LHC has been a great success. The hot pursuit for $B_s^0 \rightarrow \mu^+ \mu^-$ at the Tevatron culminated in the recent observation by the LHCb [1] and CMS [2] experiments, albeit again consistent with the Standard Model (SM). A recent combined LHC result for $B_q^0 \rightarrow \mu^+ \mu^-$ is [3],

$$\mathcal{B}(B_s^0 \rightarrow \mu^+ \mu^-) = (2.8_{-0.6}^{+0.7}) \times 10^{-9}, \quad (1.1)$$

$$\mathcal{B}(B_d^0 \rightarrow \mu^+ \mu^-) = (3.9_{-1.4}^{+1.6}) \times 10^{-10}. \quad (1.2)$$

At 6.2σ , the $B_s^0 \rightarrow \mu^+ \mu^-$ mode is established, but SM expectation is 7.6σ . The $B_d^0 \rightarrow \mu^+ \mu^-$ mode deviates from SM expectation of $(1.06 \pm 0.09) \times 10^{-10}$ [4] by 2.2σ , with central value more than 3 times the SM value. Thus, $B_d^0 \rightarrow \mu^+ \mu^-$ should be keenly followed at the up and coming LHC Run 2 (13 and 14 TeV).

For the CP violation in B_s^0 - \bar{B}_s^0 system, measured from $B_s \rightarrow f$ decay with different final states $f = J/\psi \phi$ and $f = J/\psi \phi$, a recent combined 3 fb^{-1} result given by LHCb [5] shows

$$\phi_s = -0.010 \pm 0.039, \quad (1.3)$$

with no indication of New Physics.

What are the prospects for Run 2? A total of 8 fb^{-1} or more data is expected by LHCb up to 2018. Data rate is much higher for CMS, but trigger bandwidth is an issue. Given that the two former measurables correspond to $b \leftrightarrow s$ and $b \rightarrow d$ transitions, one involving CPV, the other not, there is one particular process that comes to mind: $K \rightarrow \pi \nu \bar{\nu}$ decays, which are $s \rightarrow d$ transitions. The neutral $K_L^0 \rightarrow \pi^0 \nu \nu$ decay, pursued by the KOTO experiment [6] in Japan, is purely CPV. The charged $K^+ \rightarrow \pi^+ \nu \nu$ mode is pursued by the NA62 experiment [7] at CERN. Both experiments run within a similar time frame. If one has indications for NP in $B_q^0 \rightarrow \mu^+ \mu^-$ and/or ϕ_s , likely one would find NP in $K \rightarrow \pi \nu \bar{\nu}$, and *vice versa*. An element of competition between high- and low-energy luminosity frontiers would be quite interesting.

In this work we study the *correlations* between the measurables $B_d^0 \rightarrow \mu^+ \mu^-$, $B_s^0 \rightarrow \mu^+ \mu^-$, ϕ_s , and $K \rightarrow \pi \nu \bar{\nu}$ (especially $K_L^0 \rightarrow \pi^0 \nu \nu$), in the 4th generation (4G) model. It was pointed out quite some time ago [8] that 4G can bring about an enhanced $K_L^0 \rightarrow \pi^0 \nu \nu$, and now that KOTO is running, one should check whether it remains true. Although some may now find 4G extreme, our aim is towards enhanced $B_d^0 \rightarrow \mu^+ \mu^-$ rate by a factor of three and still survive all *flavor* constraints. The issue with 4G is the observation of a light Higgs boson, without the anticipated factor of 9 enhancement in cross section. On one hand it has been argued [9] that there still exists other interpretation of this 125 GeV boson, that is to identify it as dilaton from a 4G theory with strong Yukawa interaction. On the other hand, Higgs boson practically does not enter (i.e. is ‘‘orthogonal’’ to) low energy flavor changing processes, and, *if* one discovers an enhanced $B_d^0 \rightarrow \mu^+ \mu^-$ decay [10], it may put some doubt on the Higgs nature of the observed 125 GeV particle. We view the issue, different interpretation of this boson, is still opens and would be settled by 2018. Our 4G study serves to illustrate how New Physics in $B_q^0 \rightarrow \mu^+ \mu^-$, ϕ_s , and $K \rightarrow \pi \nu \bar{\nu}$ might be accommodated.

In what follows, we briefly introduce the scenarios and choice of input parameters, then our numerical results and end with some discussions.

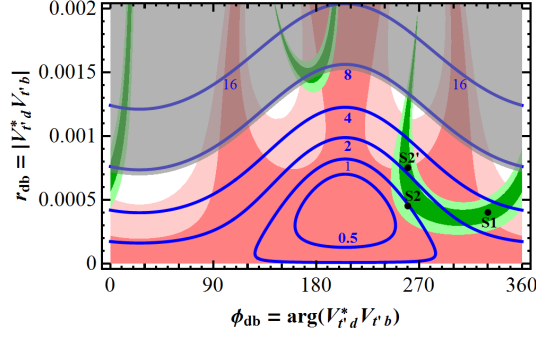


Figure 1: Update of Fig. 3(a) of Ref. [10], taking $|V_{ub}^{\text{ave}}|$ and $m_{t'} = 1000$ GeV. The pink-shaded contours correspond to $1(2)\sigma$ regions of Δm_{B_d} allowed by $f_{B_d} = (190.5 \pm 4.2)$ MeV while the green-shaded bands are for $1(2)\sigma$ in $\sin 2\beta/\phi_1 = 0.682 \pm 0.019$ [11]. Solid-blue lines are labeled $10^{10} \mathcal{B}(B_d \rightarrow \mu^+ \mu^-)$ contours, with upper bound of 7.4 [1] applied. Marked points S1, S2, S2' are explained in text.

2. Scenarios and Input Parameters

We define the parameters $x_q = m_q^2/M_W^2$, $\lambda_q^{ds} \equiv V_{qd}V_{qs}^*$ ($q = u, c, t, t'$), with

$$V_{t'd}^* V_{t's} \equiv (\lambda_{t'}^{ds})^* \equiv r_{ds} e^{i\phi_{ds}}. \quad (2.1)$$

We adopt the parametrization of Ref. [13] for the 4×4 CKM matrix, with convention and treatment of Ref. [8]. In particular, we assume SM-like values for s_{12} , s_{23} , s_{13} and $\phi_{ub} \simeq \gamma/\phi_3$, with following input: $|V_{us}| = 0.2252 \pm 0.0009$, $|V_{cb}| = 0.0409 \pm 0.0011$, $|V_{ub}^{\text{ave}}| = (4.15 \pm 0.49) \times 10^{-3}$, $\gamma/\phi_3 = (68_{-11}^{+10})^\circ$. This is a simplification, since we try to observe trends, rather than making a full fit. We find taking the ‘‘exclusive’’ measurement value for $|V_{ub}|$ allows less enhancement range for $K_L \rightarrow \pi^0 \nu \bar{\nu}$.

Having a 4th generation of quarks brings in three new angles and two new phases. In this paper, we take

$$m_{t'} = 1000 \text{ GeV}, \quad s_{34} \simeq m_W/m_{t'} \simeq 0.08, \quad (2.2)$$

for sake of illustration, thereby fixing one of the angles. A second angle and one of the two phases are fixed by the discussion illustrated below. We are then left with two mixing parameters, and for our interest in $K \rightarrow \pi \nu \bar{\nu}$ decays, we take as r_{ds} and ϕ_{ds} in Eq. (2.1).

In Fig. 1, we update Fig. 3(a) of Ref. [10] on the $r_{db}-\phi_{db}$ plane, where $V_{t'd}^* V_{t'b} \equiv r_{db} e^{i\phi_{db}}$ using latest input parameters, see [12]. Two scenarios, marked as S1 and S2,

$$r_{db} e^{i\phi_{db}} = 0.00040 e^{i330^\circ}, \quad 0.00045 e^{i260^\circ}, \quad (2.3)$$

is imposed to illustrate

$$\mathcal{B}(B_d \rightarrow \mu^+ \mu^-) \sim 3 \times 10^{-10}, \quad 1 \times 10^{-10}, \quad (2.4)$$

where we stay within 1σ boundaries of both Δm_{B_d} (uncertainty in f_{B_d}) and $\sin 2\beta/\phi_1$. $B_d \rightarrow \mu^+ \mu^-$ is SM-like for S2, but carries a near maximal $4G$ CPV phase ϕ_{db} . The point S2' will be discussed towards the end.

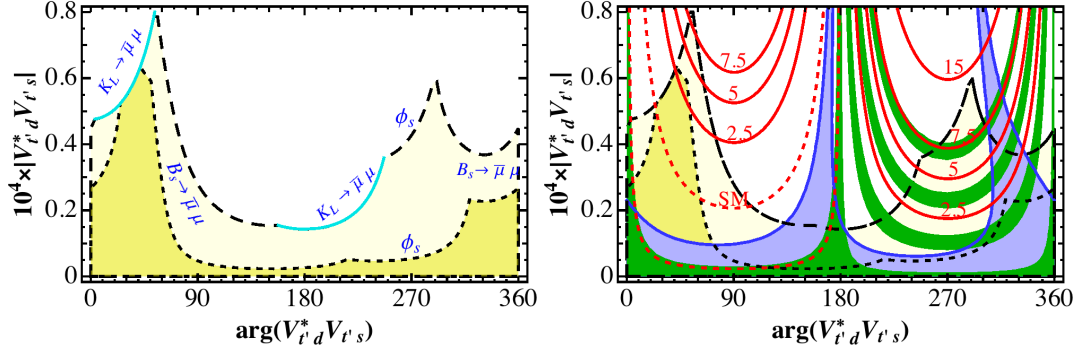


Figure 2: [left] Allowed region in $|V_{t'd}^* V_{t's}| - \arg(V_{t'd}^* V_{t's})$ (i.e. $r_{ds} - \phi_{ds}$) plane for Scenario S1, $r_{db} e^{i\phi_{db}} = 0.0004 e^{i330^\circ}$ (enhanced $B_d \rightarrow \mu^+ \mu^-$) and $\phi_s = -0.010 \pm 0.039$ where the constraint source for each boundary is indicated. The leading constraint is $B_s \rightarrow \mu^+ \mu^-$, where $1(2)\sigma$ region — towards larger (smaller) BR in central region (4th-extending-to-1st quadrants) — is (very) light shaded, separated by dashed lines, except: $K_L \rightarrow \mu^+ \mu^-$ cuts off at upper left, as well as center-right, indicated by light-blue solid lines; $1(2)\sigma$ allowed ϕ_s cuts off the $1(2)\sigma$ allowed $B_s \rightarrow \mu^+ \mu^-$ in right-center, plus a sliver in 1st quadrant. [right] The allowed region is further overlaid with ϵ_K (blue-shaded), ϵ'/ϵ (narrow green bands corresponding to R_6 in increasing order from 1.0, 1.5, 2.0, 2.5) and $\mathcal{B}(K_L \rightarrow \pi^0 \nu \bar{\nu})$, labeled in 10^{-10} units. The illustration is for $m_{t'} = 1000$ GeV (Eq. (11)).

Without involving detailed formulas and inputs of relevant observables on hand, which can be referred to [12] as well, we straightforwardly present our numerical results in below.

3. Results

To illustrate the connection between $B_d \rightarrow \mu^+ \mu^-$ and $K_L \rightarrow \pi^0 \nu \bar{\nu}$, we explore two scenarios (see Fig. 1):

- Scenario S1: $r_{db} e^{i\phi_{db}} = 0.00040 e^{i330^\circ}$
 $\mathcal{B}(B_d \rightarrow \mu^+ \mu^-) \gtrsim 3 \times \text{SM}$, with $e^{i\phi_{db}}$ complex;
- Scenario S2: $r_{db} e^{i\phi_{db}} = 0.00045 e^{i260^\circ}$
 $\mathcal{B}(B_d \rightarrow \mu^+ \mu^-) \sim \text{SM}$, ϕ_{db} is near maximal CPV;

In both scenarios, ϕ_s is well within range of the 3 fb^{-1} result of LHCb, Eq. (1.3).

We plot in Fig. 2[left] the region in the $|V_{t'd}^* V_{t's}| - \arg(V_{t'd}^* V_{t's})$ or $r_{ds} - \phi_{ds}$ plane allowed by various constraints for S1. The golden-hued (very) light shaded regions are for $1(2)\sigma$ of the $B_s \rightarrow \mu^+ \mu^-$ mode. Other constraints, labeled by the process, cut in at certain regions: $\mathcal{B}(K_L \rightarrow \mu \mu)_{\text{SD}}$ at the upper-left corner, and just right of center; $\phi_s = -0.049(-0.088)$ at $1(2)\sigma$ cuts off near center of right-hand side, and a tiny sliver in first quadrant. The remaining 1σ contours for $B_s \rightarrow \mu^+ \mu^-$ correspond to 3.5×10^{-9} (central-left region) and 2.2×10^{-9} (4th quadrant extending into 1st quadrant) in rate, and for 2σ contours, 4.3×10^{-9} [3] from 1st to 2nd quadrant and 1.6×10^{-9} in 4th quadrant only. We find that $R = \Delta m_{B_d} / \Delta m_{B_s}$ does not provide further constraint within 2σ .

The allowed region of Fig. 2[left] is further overlaid, in Fig. 2[right], by the constraints of ϵ_K , ϵ'/ϵ , and give $K_L \rightarrow \pi^0 \nu \bar{\nu}$ contours in red-solid, labeled by BR values in 10^{-10} units. Note that

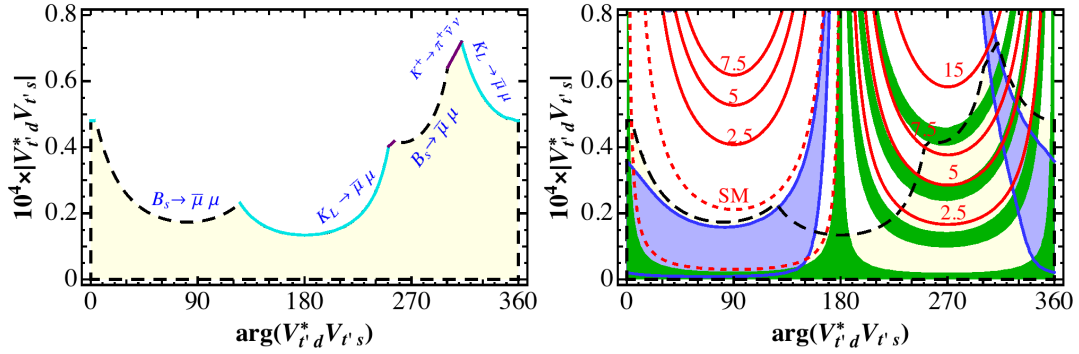


Figure 3: Scenario S2, $r_{db} e^{i\phi_{db}} = 0.00045 e^{i260^\circ}$ (SM-like $B_d \rightarrow \mu^+ \mu^-$): [left] Similar to Fig. 2a, where for the 4th quadrant of interest, the 2σ dashed line is for $B_s \rightarrow \mu^+ \mu^-$ and solid is for $K_L \rightarrow \mu^+ \mu^-$ (plus a bit from $K^+ \rightarrow \pi^+ \nu \bar{\nu}$); [right] Similar to Fig. 2b, with ϵ_K (blue-shaded) ϵ'/ϵ (green bands) and $K_L \rightarrow \pi^0 \nu \bar{\nu}$ (red labelled contours) overlaid.

“15” is just above the nominal GN bound, while the region \lesssim SM strength is marked by red-dash lines with label “SM”. The ϵ_K constraint, plotted in shaded blue with theoretical error (experimental error negligible), prefers small $|V_{t'd}^* V_{t's}|$ values, except two “chimneys” where the phase of $V_{t'd}^* V_{t's}$ is small for one near 180° , and the other is tilted in the fourth quadrant. The ϵ'/ϵ constraint is more subtle, because of the less known [14] hadronic parameter R_6 (we fix $R_8 \simeq 0.7$ [15]). We illustrate [8] with $R_6 = 1.0, 1.5, 2.0, 2.5$, in ascending order of green bands determined by experimental error of ϵ'/ϵ .

First, we observe that the ϵ_K and ϵ'/ϵ constraints disfavor the possible enhancements for $K_L \rightarrow \pi^0 \nu \bar{\nu}$ when $\arg(V_{t'd}^* V_{t's})$ is in the first two quadrants. Second, if one keeps all constraints to 1σ , then $K_L \rightarrow \pi^0 \nu \bar{\nu}$ could reach a factor ~ 7 above SM, with modest R_6 values. However, if one allows larger R_6 (up to 2.5) as well as 2σ variations, the ϵ_K “chimney” in the 4th quadrant allows $K_L \rightarrow \pi^0 \nu \bar{\nu}$ to be enhanced up to $1/3$, even $1/2$, the GN bound. There is a correlation between larger $K_L \rightarrow \pi^0 \nu \bar{\nu}$ and smaller $B_s \rightarrow \mu\mu$. If KOTO observes $K_L \rightarrow \pi^0 \nu \bar{\nu}$ shortly after reaching below the GN bound, a rather large R_6 value could be implied. One argument for larger $K_L \rightarrow \pi^0 \nu \bar{\nu}$ or smaller $B_s \rightarrow \mu\mu$ is for larger values of $|V_{t'd}^* V_{t's}|$: since $|V_{t'd}| \sim 0.005$, to have $|V_{t's}| > |V_{t'd}|$ would demand $|V_{t'd}^* V_{t's}| \gtrsim 0.25 \times 10^{-4}$.

For Scenario S2, where $B_d \rightarrow \mu\mu$ is taken as consistent with SM, but $\phi_{db} \equiv \arg(V_{t'd}^* V_{t'b}) \simeq 260^\circ$ is close to maximal CPV phase (in our convention, $V_{t'b}$ is real) with $K_L \rightarrow \pi^0 \nu \bar{\nu}$ in mind, we plot in Fig. 3[left] the results corresponding to Fig. 2[left]. The regions marked by long dashed lines and very lightly shaded are all beyond 1σ level, indicating more tension, including in $R = \Delta m_{B_d} / \Delta m_{B_s}$. The $B_s \rightarrow \mu\mu$ constraint at 2σ is interspersed with the $\mathcal{B}(K_L \rightarrow \mu\mu)_{SD}$ constraint, plus short segments from $K^+ \rightarrow \pi^+ \nu \bar{\nu}$. As in Fig. 2[right], we overlay the constraints of ϵ_K , ϵ'/ϵ , as well as $K_L \rightarrow \pi^0 \nu \bar{\nu}$ contours, in Fig. 3[right]. Again, $K_L \rightarrow \pi^0 \nu \bar{\nu}$ cannot get enhanced in first two quadrants. For the blue-shaded “chimney” in 4th quadrant, as the R_6 value rises, $K_L \rightarrow \pi^0 \nu \bar{\nu}$ could get enhanced even up to GN bound, but $B_s \rightarrow \mu\mu$ would become relatively suppressed, and there is some tension with SD contribution to $K_L \rightarrow \mu\mu$. Note that $\mathcal{B}(B_d \rightarrow \mu\mu) \sim$ SM in this case. Here, having $|V_{t's}| > |V_{t'd}|$ would demand $|V_{t'd}^* V_{t's}| \gtrsim 0.32 \times 10^{-4}$, hence in favor of larger $K_L \rightarrow \pi^0 \nu \bar{\nu}$.

We have marked a point S2' in Fig. 1, which has same $\phi_{db} \simeq 260^\circ$ as S2, but enhances $B_d \rightarrow \mu\mu$

by a larger $r_{db} \equiv |V_{t'd}^* V_{t'b}| \simeq 0.00075$. The trouble with S2' is that $\Delta m_{B_d}/\Delta m_{B_s}$ ratio becomes inconsistent at 2σ level, which we do not consider as viable. However, from S2 towards S2', one could enhance $B_d \rightarrow \mu\mu$ while $K_L \rightarrow \pi^0 \nu \bar{\nu}$ is more easily enhanced up to GN bound. The cost would be some tension in $\Delta m_{B_d}/\Delta m_{B_s}$.

4. Discussion and Conclusion

We are interested in the correlation between $B_d \rightarrow \mu^+ \mu^-$ and $K_L \rightarrow \pi^0 \nu \bar{\nu}$ in 4G, as constrained by $B_s \rightarrow \mu\mu$ and ϕ_s . Scenario S1 illustrates enhanced $B_d \rightarrow \mu^+ \mu^-$ with generic $V_{t'd}^* V_{t'b}$. Every measurement other than $B_d \rightarrow \mu^+ \mu^-$ would be close to SM expectation, and a mild enhancement of $K_L \rightarrow \pi^0 \nu \bar{\nu}$ is possible. But it would take some while for KOTO to reach this sensitivity. Larger $K_L \rightarrow \pi^0 \nu \bar{\nu}$ correlates with smaller $B_s \rightarrow \mu^+ \mu^-$, as well as larger hadronic parameter R_6 . The ϕ_s constraint basically suppresses the phase of $V_{t'd}^* V_{t'b}$.

It could happen that $B_d \rightarrow \mu^+ \mu^-$ ends up SM-like, which is illustrated by Scenario S2. In the 4G framework that accounts (within 1σ) for the $\sin 2\beta/\phi_1$ ‘‘anomaly’’, this occurs when $\phi_{db} \equiv \arg(V_{t'd}^* V_{t'b})$ phase is near maximal, which is of interest for enhancing $K_L \rightarrow \pi^0 \nu \bar{\nu}$, a purely CPV process. We find that $K_L \rightarrow \pi^0 \nu \bar{\nu}$ can be enhanced up to practically the GN bound at the cost of large R_6 , while staying within the ϕ_s constraint. There is the same correlation of larger $K_L \rightarrow \pi^0 \nu \bar{\nu}$ for smaller $B_s \rightarrow \mu^+ \mu^-$. While the S2' point would push $\Delta m_{B_d}/\Delta m_{B_s}$ beyond 2σ tolerance, some $|V_{t'd}^* V_{t'b}| \equiv r_{db}$ value below 0.00075 could still enhance $B_d \rightarrow \mu^+ \mu^-$ a bit from SM, but $K_L \rightarrow \pi^0 \nu \bar{\nu}$ can more easily saturate the Grossman-Nir bound, with implication that $K^+ \rightarrow \pi^+ \nu \bar{\nu}$ is towards the large side allowed by E949, $B_s \rightarrow \mu\mu$ is visibly suppressed, while R_6 must be sizable. This would clearly be a bonanza situation for faster discovery!

We have used 4G for illustration [16], since it supplies $V_{t's}$ and $V_{t'd}$ that affect $b \rightarrow s$ and $b \rightarrow d$ transitions, and induces correlations with $s \rightarrow d$ transitions. It is generally viewed that the fourth generation is ruled out by the SM-like Higgs boson production cross section. But we have argued [10] that the Higgs boson does not enter the low energy processes discussed here, hence these processes are independent *flavor* checks. Furthermore, loopholes exist for the SM-Higgs interpretation [9]. The modes $B_{d,s} \rightarrow \mu^+ \mu^-$, ϕ_s and $K_L \rightarrow \pi^0 \nu \bar{\nu}$ provide ‘‘pressure tests’’ to our understanding of flavor and CP violation, where genuine surprises may emerge. Though differences must exist, we believe there would be correlations between the above four modes in any New Physics model with a limited set of new parameters. The NA62 experiment has started [7] running. If $K^+ \rightarrow \pi^+ \nu \bar{\nu}$ turns out to be above the 90% CL limit from E949, the GN bound for $K_L \rightarrow \pi^0 \nu \bar{\nu}$ moves up, making things more interesting for KOTO, where the aim [6] for the 2015 run is to reach the GN bound around 1.4×10^{-9} .

In conclusion, enhanced $B_d^0 \rightarrow \mu^+ \mu^-$ could correlate with enhanced $K_L \rightarrow \pi^0 \nu \bar{\nu}$ up to the Grossman-Nir bound in the 4th generation model. $B_s^0 \rightarrow \mu^+ \mu^-$ becomes somewhat suppressed, with CPV phase $\phi_s \simeq 0$. Together with $K^+ \rightarrow \pi^+ \nu \bar{\nu}$, these measurements would provide ‘‘pressure tests’’ to our understanding of flavor and CP violation for any New Physics model. They should be followed earnestly in parallel to the scrutiny of the nature of the 125 GeV boson at LHC Run 2.

References

- [1] R. Aaij *et al.* [LHCb Collaboration], Phys. Rev. Lett. **111**, 101805 (2013).

- [2] S. Chatrchyan *et al.* [CMS Collaboration], Phys. Rev. Lett. **111**, 101804 (2013).
- [3] V. Khachatryan *et al.* [CMS and LHCb Collaborations], arXiv:1411.4413 [hep-ex], accepted to *Nature*.
- [4] C. Bobeth *et al.*, Phys. Rev. Lett. **112**, 101801 (2014).
- [5] R. Aaij *et al.* [LHCb Collaboration], Phys. Rev. Lett. **114**, 041801 (2015).
- [6] T. Nomura, talk at ICHEP 2014, Valencia, Spain, July 2014.
- [7] A. Sergi, talk at ICHEP 2014, Valencia, Spain, July 2014.
- [8] W.-S. Hou, M. Nagashima, A. Soddu, Phys. Rev. D **72**, 115007 (2005).
- [9] For a possible interpretation, see e.g. Y. Mimura, W.-S. Hou, H. Kohyama, JHEP **1311**, 048 (2013).
- [10] W.-S. Hou, M. Kohda, F. Xu, Phys. Rev. D **87**, 094005 (2013).
- [11] Y. Amhis *et al.* [Heavy Flavor Averaging Group], <http://www.slac.stanford.edu/xorg/hfag>.
- [12] W. S. Hou, M. Kohda and F. Xu, arXiv:1411.1988 [hep-ph].
- [13] W.-S. Hou, A. Soni, H. Steger, Phys. Lett. B **192**, 441 (1987).
- [14] An example for a large R_6 value can be found in J. Bijnens and J. Prades, JHEP **0006**, 035 (2000).
- [15] T. Blum *et al.*, Phys. Rev. D **86**, 074513 (2012).
- [16] The t' mass is large, but always come with CKM factors, hence remains perturbative. The loop functions may be modified by the strong Yukawa coupling, but our purpose to illustrate the power of CKM4 should remain valid.